University of Miskolc

Torque Optimization of Sucker-Rod Pumping Units

New scientific achievements of PhD Thesis

László Kis

Petroleum and natural gas engineer

University of Miskolc, Petroleum and Natural Gas Institute

Mikoviny Sámuel Doctoral School of Earth Sciences
Head of the doctoral school: Prof. Dr. Péter Szűcs, professor

Fluid production and transporting research section
Head of the section: Prof. Dr. László Tihanyi, professor emeritus

Integrated petroleum and natural gas production systems topic
Head of the topic: Prof. Dr. Gábor Takács, professor emeritus

Advisor: ***Prof. Dr. Gábor Takács, professor emeritus***

Miskolc, 2021

INTRODUCTION

The initial objective of the presented thesis was the investigation of the effect of using asymmetrical counterweight configuration in the counterbalancing of crank balanced sucker-rod pumping units. Before the optimization of the net gearbox torque can be carried out, the knowledge of all distinct torque components acting on the gearbox throughout the pumping cycle is necessary to accurately describe the actual torque conditions of the investigated pumping unit. The improved torque analysis presented in this work is based on the data provided by an electronic dynamometer, the routinely used measurement tool for sucker-rod pumping units. After studying the API Spec 11E (API, 2013) – the recommendation by the American Petroleum Institute – it became apparent, that it lacks the capability to describe those sucker-rod pumping units that have varying crank angular velocities throughout their pumping cycle accurately.

The second objective of the research was to develop a calculation method to optimize the mechanical net gearbox torque and to determine the corresponding counterweight configuration for the investigated sucker-rod pumping unit. By properly considering the effect of the asymmetrically placed counterweights, the number of independent variables increases from three – in the case of symmetrical counterweight configuration – to twelve; which makes the direct determination of the optimal arrangement of the counterweights impossible. Therefore, a particle swarm optimization (PSO) algorithm was used, due to the size of the solution space. The asymmetrically placed counterweights not only change the counterbalance torque by introducing a secondary phase angle but will alter both the rotary inertial torques as well. A computer program has been developed to handle the interpretation of the dynamometer surveys.

NEW SCIENTIFIC ACHIEVEMENTS

THESIS 1

A successive approximation procedure is presented that produces the crank angle values corresponding to the measured polished rod positions with a higher accuracy than previously existing methods. Since the crank angle variation in time is not measured by a dynamometer survey, it must be calculated from the measured polished rod positions and the kinematic parameters of the sucker-rod pumping unit. The exact calculation procedure developed here has a high importance because any errors in the crank angle vs time function affect almost every other parameter in the evaluation of the torque conditions of sucker rod pumping units. By minimizing the error in the first calculation step, the accuracy of torque calculations as well as counterbalance optimizations are improved.

The flowchart of the calculation procedure developed is shown in Figure 1, its subroutines are shown in Figure 2. Using this procedure, the crank angle values can be determined for cases when the crankshaft turns at variable rotational speeds.

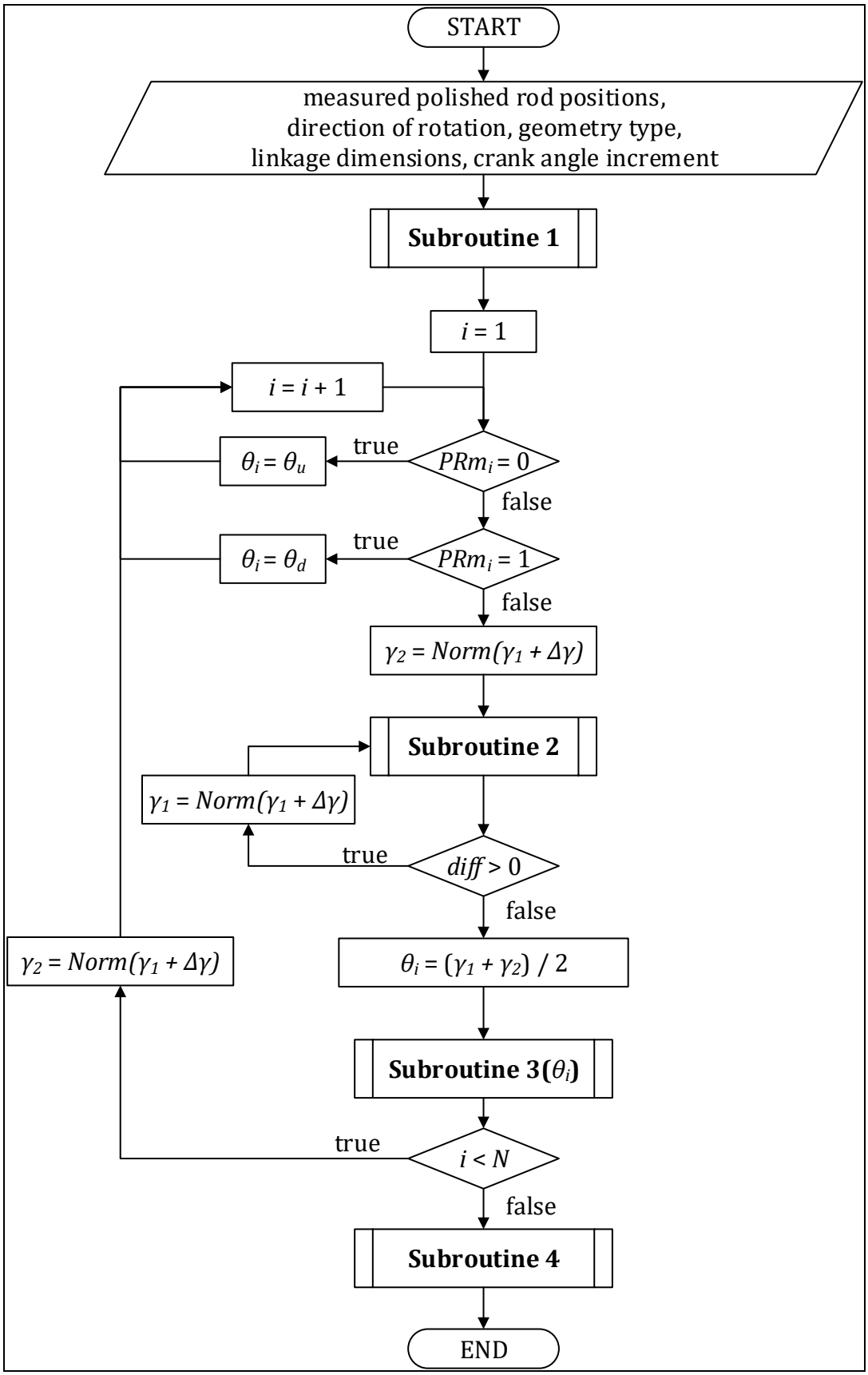

Figure 1 *Flowchart of the successive approximation numerical method that finds the crank angles corresponding to the measured polished rod positions*

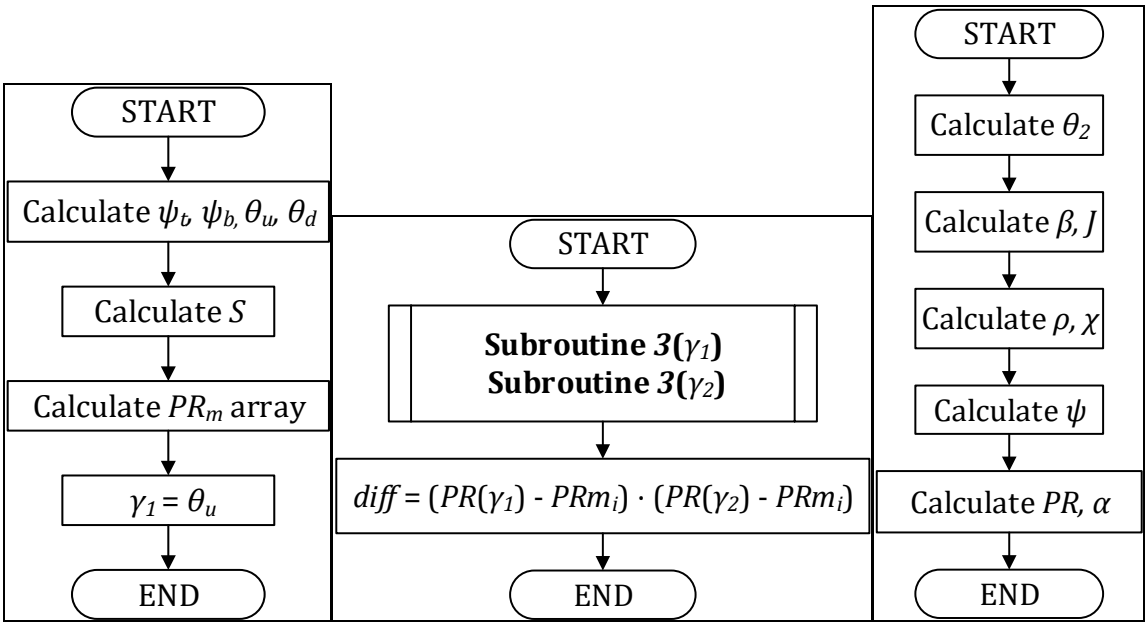

Figure 2 *Subroutines 1-3 of the successive approximation numerical method*

THESIS 2

A complex calculation method was developed that produces the crank angular velocity, the crank angular acceleration, and the beam angular acceleration variation throughout the pumping cycle. The proposed method has superior precision compared to the most widely used software in the industry. The numerical calculation models presented have proved to be strong validating tools to help verify the results of the more complex, but cumbersome calculation methods.

The calculation process includes the use of truncated Fourier series on the numerically calculated crank angular velocities. The flowchart of the procedure is shown in Figure 3. The raw data needed transformation for the determination of the coefficients using the following formulae shown below.

$$t_{F_i} = \frac{i \cdot T}{N}$$

where:

t_{F_i}	i[th] element of the Fourier time array [sec],
i	Index that goes from *0* to *N-1* [-], and
N	Number of measured data points [-].

$$d_{F_i} = d_i + (d_i - d_{i-1}) \cdot \frac{t_{F_i} - t_i}{t_i - t_{i-1}}$$

where:

d_{F_i}	i[th] element of the Fourier input data array [var.],
d_i	i[th] element of the data array [var.],
t_{F_i}	i[th] element of the Fourier time array [sec], and
t_i	i[th] element of the measured time array [sec].

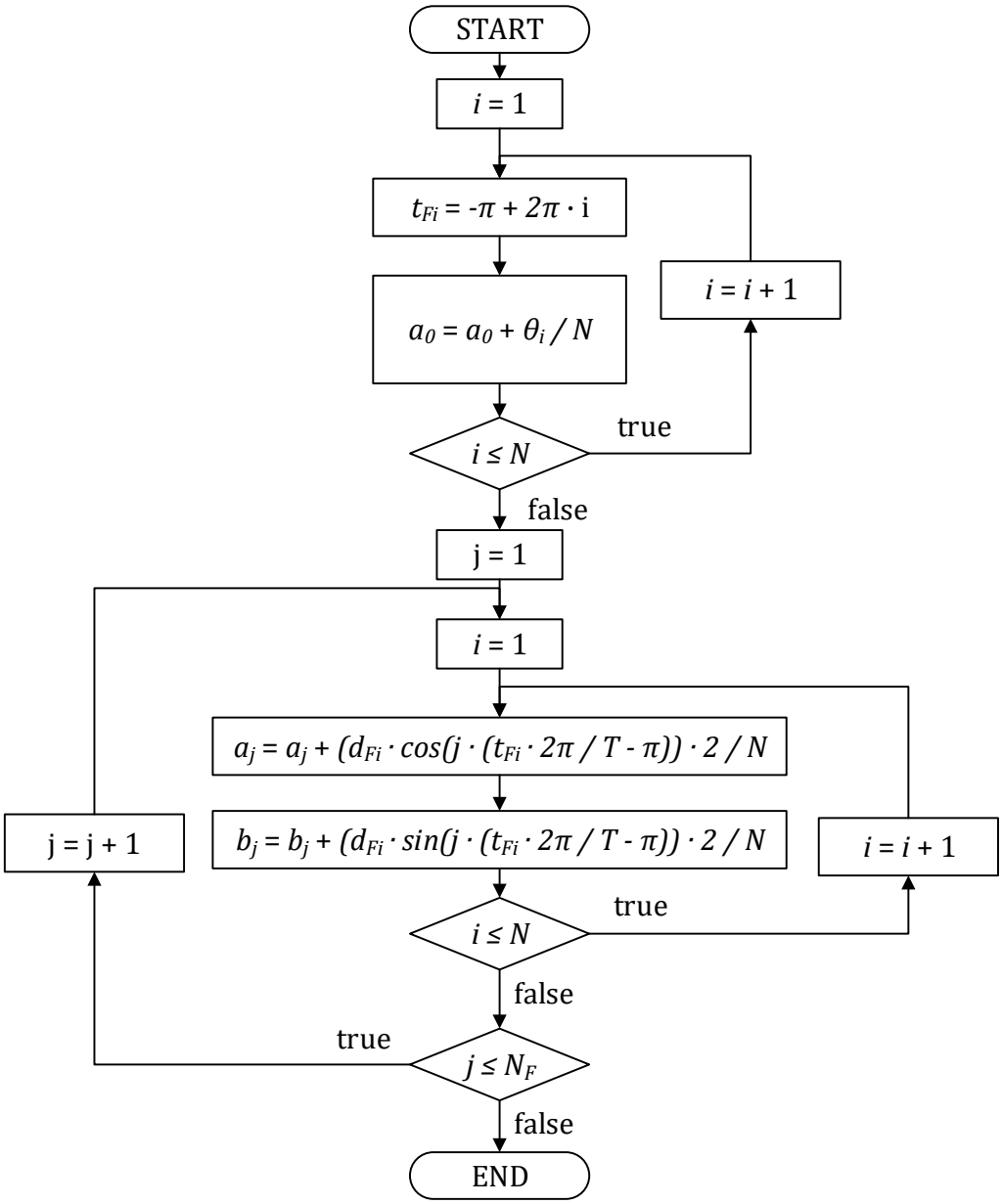

Figure 3 *Flowchart of determining the Fourier coefficients*

Once the coefficients are determined the Fourier function along with its derivatives are determined using the following equations.

$$F_i = a_0 + \sum_{k=1}^{N_F} a_k \cdot \cos\left(\left(\frac{2\pi \cdot t_i}{T} - \pi\right) \cdot k\right) + b_k \cdot \sin\left(\left(\frac{2\pi \cdot t_i}{T} - \pi\right) \cdot k\right)$$

where:

F_i	i[th] solution of the Fourier series at the measured times [var.],
a_0	Constant coefficient of the Fourier series [-],
a_k, b_k	k[th] coefficients of the Fourier series [-],
t_i	i[th] element of the measured time array [sec],
T	Period time [sec],
k	Index of the coefficients in the Fourier series [-], and
N_F	Number of coefficients in the Fourier series [-].

$$\frac{\mathrm{d}F}{\mathrm{d}t}_i = \frac{2\cdot\pi}{T}\cdot\sum_{k=1}^{N_F} -a_k\cdot\sin\left(\left(\frac{2\pi\cdot t_i}{T}-\pi\right)\cdot k\right)+b_k\cdot cos\left(\left(\frac{2\pi\cdot t_i}{T}-\pi\right)\cdot k\right)$$

$$\frac{\mathrm{d}^2F}{\mathrm{d}t^2}_i = \frac{-4\cdot\pi^2}{T^2}\cdot\sum_{k=1}^{N_F} a_k\cdot\cos\left(\left(\frac{2\pi\cdot t_i}{T}-\pi\right)\cdot k\right)+b_k\cdot sin\left(\left(\frac{2\pi\cdot t_i}{T}-\pi\right)\cdot k\right)$$

The Fourier series cannot be used directly on the calculated crank angle array, because it has a discontinuity due to its definition. Therefore, the crank angular velocity values had to determined numerically first. An advanced numerical differentiation was used to improve the accuracy of the resulting Fourier function, see the equation below.

$$\frac{\Delta\theta}{\Delta\mathrm{t}}_{num2_i} = \frac{Norm(-\theta_{i+2}+8\cdot\theta_{i+1}-8\cdot\theta_{i-1}+\theta_{i-2})}{12\cdot(t_{i+1}-t_i)}$$

where:

$\frac{\Delta\theta}{\Delta\mathrm{t}}_{num2_i}$ Numerically calculated crank angular velocity using the five-step stencil method [rad/sec],

θ_i i[th] element of the calculated crank angle array [rad], and

t_i i[th] element of the measured time array [sec].

Figure 4 and Figure 5 show the calculated crank angular velocity and crank angular acceleration functions, respectively.

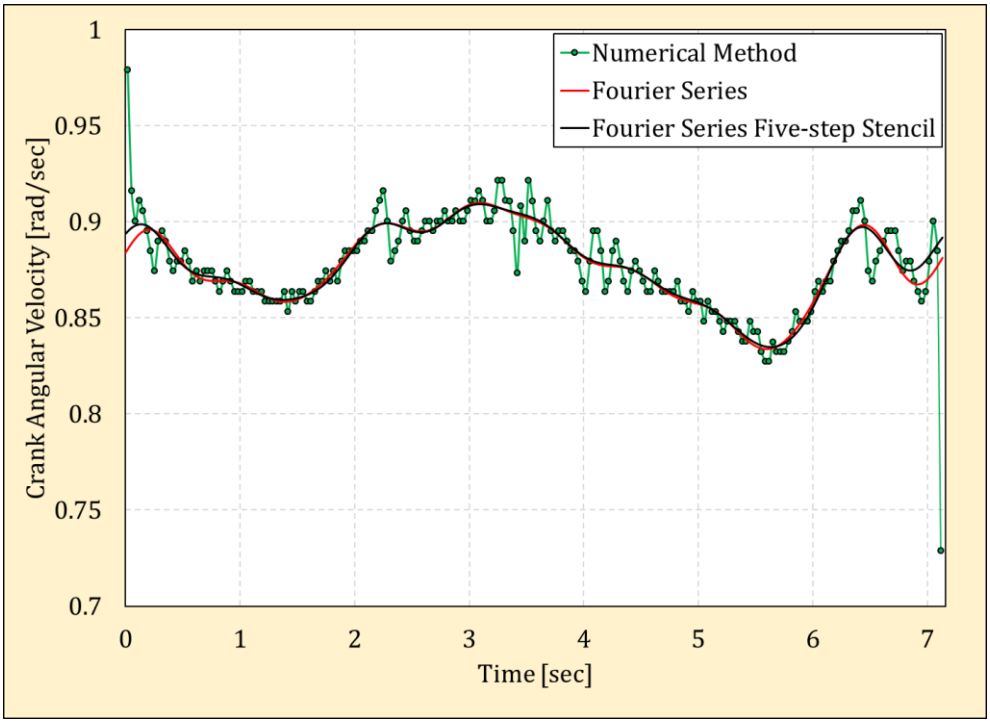

Figure 4 *The calculated crank angular velocity function*

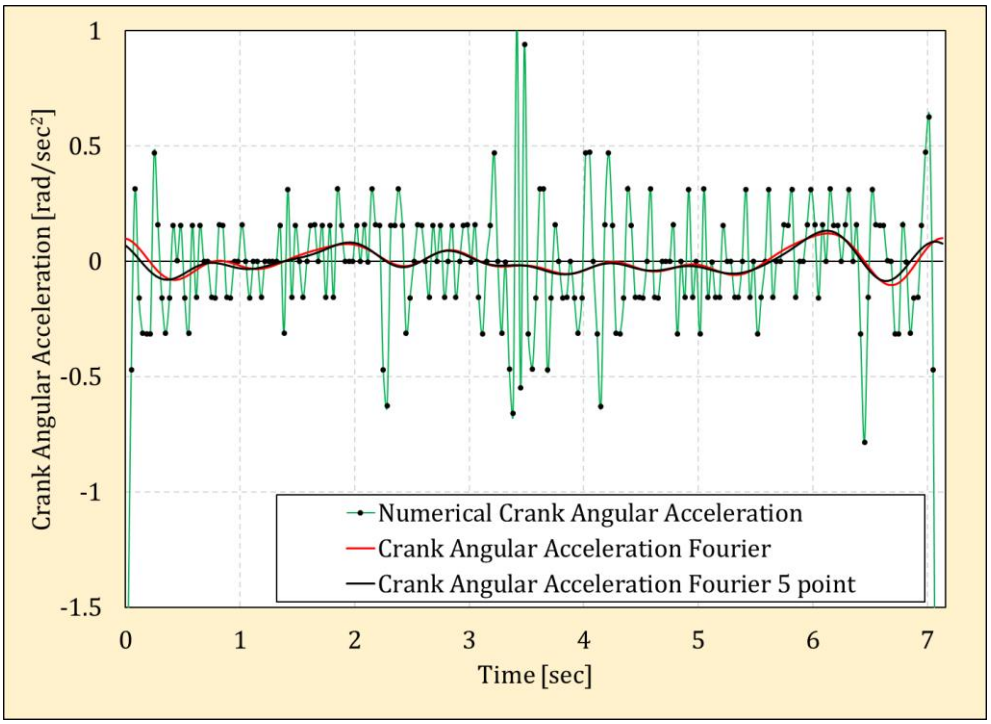

Figure 5 *The calculated crank angular acceleration function*

The angular acceleration pattern of the walking beam was determined by three different methods: a numerical method, the Svinos method and the procedure proposed by Gibbs; their results are shown in Figure 6. (Svinos, 1983) (Gibbs, 1975)

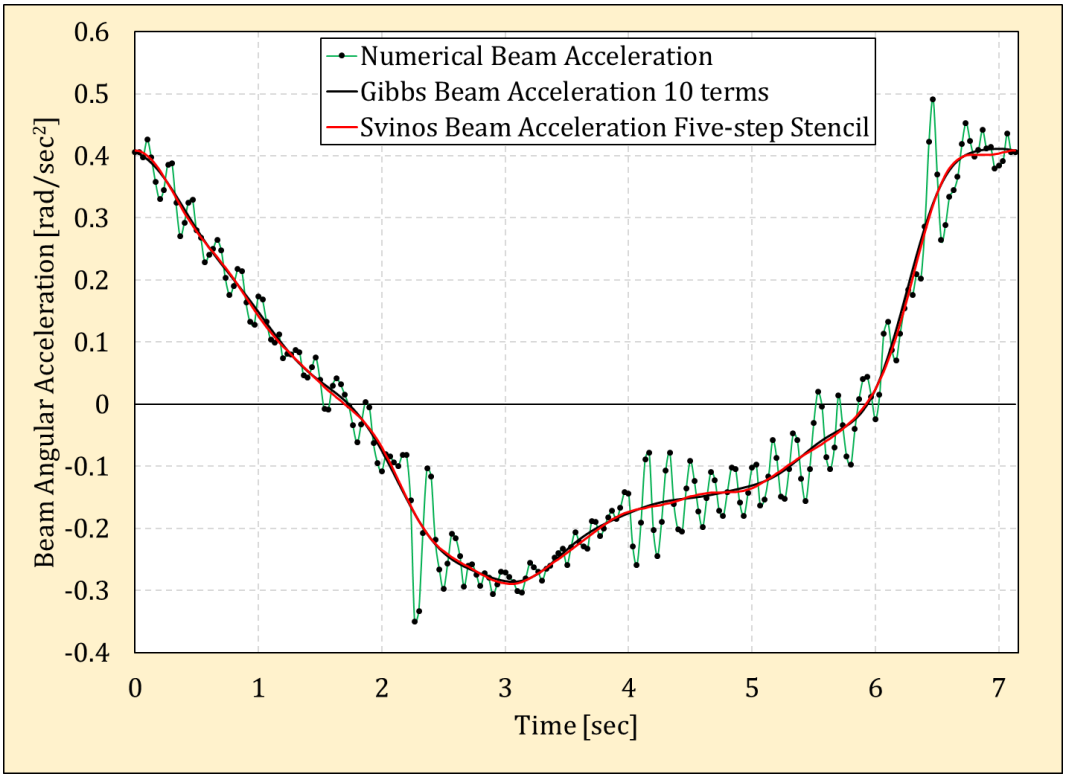

Figure 6 *Comparison of models calculating the beam angular acceleration*

THESIS 3

The effects of asymmetrical counterweight configurations on the counterbalance torque vs time function were investigated; that is an often ignored condition in the professional literature. Asymmetrical counterweight placement affects the net gearbox torque variation in time. In this work a secondary phase angle – τ' – was introduced to adequately describe the deviation of the counterbalance torque from the symmetrical cases. The new equations developed permit the accurate calculation of inertial torques and were incorporated in the gearbox torque optimization procedures introduced. The following equations define the counterbalance torque function and the secondary phase angle, respectively.

$$T_{CB}(t) = -T_{CBMax} \cdot sin(\theta(t) + \tau + \tau')$$

where:

T_{CBMax}	Maximum counterbalance moment [in lb],
$\theta(t)$	Crank angle variation in time [rad],
τ	Phase angle [rad], and
τ'	Secondary phase angle [rad].

$$\tau' = tan^{-1}\left(\frac{Y}{X}\right)$$

where:

Y	Vertical distance of the center of gravity of the system containing the cranks and the counterweights from the crankshaft [in], and
X	Horizontal distance of the center of gravity of the system containing the cranks and the counterweights from the crankshaft [in].

In the following recommended equations, the coordinates of the combined center of gravity of the system containing the crank arms and counterweights are defined. Using these values, the secondary phase angle can be determined.

$$X = \frac{X_{cr} \cdot m_{cr} + \sum_{i=1}^{n}\left(X_{cw_i} \cdot \left(m_{cw_i} + \sum_{j=1}^{n_{a_i}} m_{cw_{a_{i_j}}}\right)\right)}{m_{cr} + \sum_{i=1}^{n}\left(m_{cw_i} + \sum_{j=1}^{n_{a_i}} m_{cw_{a_{i_j}}}\right)}$$

where:

X_{cr}	Horizontal distance of the center of gravity of the crank from the crankshaft [in],
m_{cr}	Mass of the crank arm [lb_m],
X_{cw_i}	Horizontal distance of the center of gravity of the i^{th} counterweight from the crankshaft [in],
m_{cw_i}	Mass of the i^{th} counterweight [lb_m], and
$m_{cw_{a_{i_j}}}$	Mass of the j^{th} auxiliary weight on the i^{th} counterweight [lb_m].

$$Y = \frac{\sum_{i=1}^{n}(-1)^n \cdot \left((Y_{cw_i} + HW_{cr}) \cdot \left(m_{cw_i} + \sum_{j=1}^{n_{a_i}} m_{cw_{a_{ij}}} \right) \right)}{m_{cr} + \sum_{i=1}^{n} \left(m_{cw_i} + \sum_{j=1}^{n_{a_i}} m_{cw_{a_{ij}}} \right)}$$

where:

Y_{cw_i} Vertical distance of the center of gravity of the i[th] counterweight from its base [in].

Figure 7 shows the connection between the combined center of gravity and the secondary phase angle for asymmetrical counterweight configurations. The use of different counterweight types on the opposing edges of the crank arm will not only change the amplitude of the counterbalance torque, but will shift the counterbalance torque with the resulting secondary phase angle as shown in Figure 8.

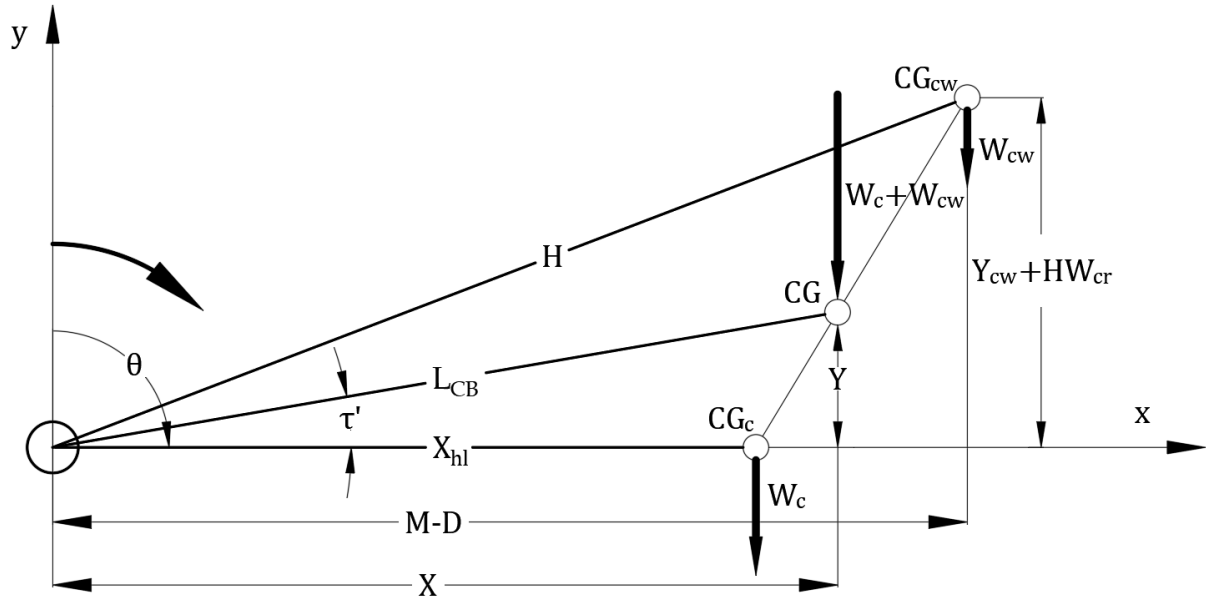

Figure 7 *Illustration of the center of gravity change due to asymmetrical counterbalancing*

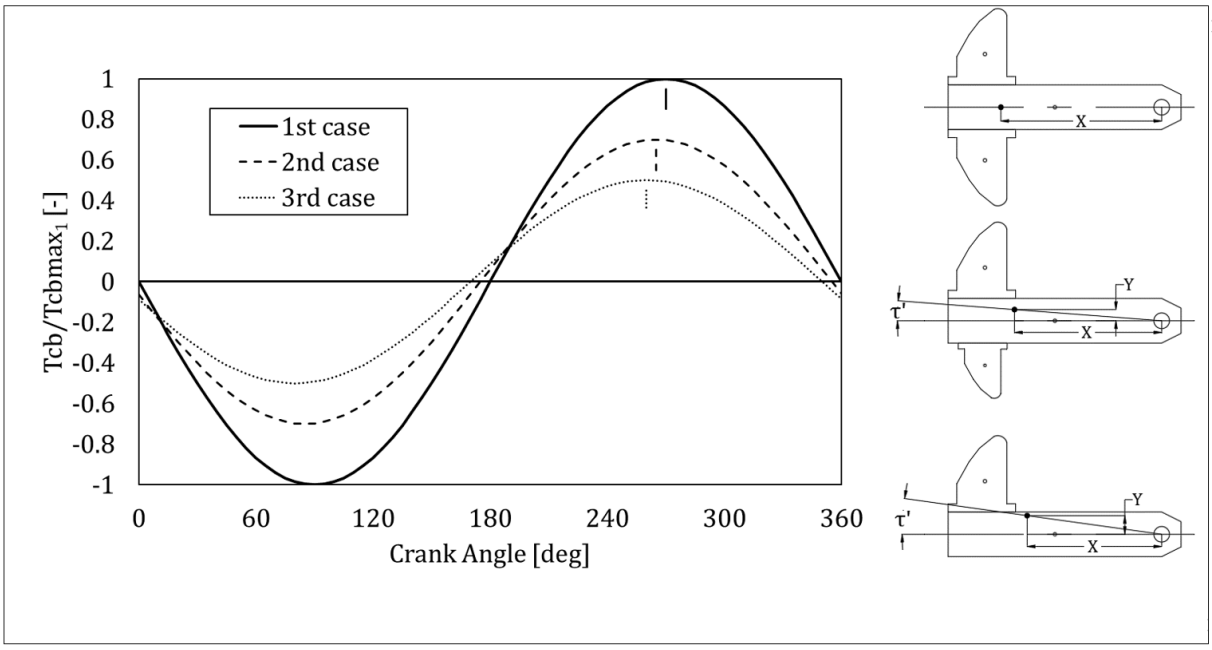

Figure 8 *Effect of different asymmetrical counterweight configurations on the counterbalance torque function*

THESIS 4

A novel technique to solve the optimization of gearbox torque conditions was developed using the particle swarm optimization (PSO) method. The calculation procedure can be used for both symmetrical and asymmetrical counterweight configurations. It can perform optimizations for different scenarios: minimizing the peak net torque or the cyclic load factor (CLF) values. As proved in this work, use of asymmetrical counterweight placements can significantly reduce the peak net gearbox torque; an often overlooked practice in the oil field.

The use of a PSO technique is preferred, when the direct calculation of the optimum condition is not possible, and when the other multi-dimensional optimization algorithms fail to find the global optimum. This can happen because of the high number of local optima in the solution space, or when the fitness function is not continuously differentiable. The flexibility of this method is its strongest advantage compared to other algorithms. The general optimization method can be customized with little effort to the solve the task at hand effectively by either modifying the calculation procedure, or changing the parameters used in the method to create an improved optimization process. (Eberhart & Kennedy, 2001)

The method uses a given number of candidates – called a swarm of particles – and improves their position in the solution space in each calculation step. Each particle is defined by a vector; its coordinates define the position of the particle in the respective dimensions of the solution space. The dimension of the required vector is determined by the number of independent variables used in the optimization procedure. The determination of the new positions is carried out by minimizing the fitness – an error function value – of the particles. The visualization of this step-by-step improvement shows remarkable resemblance to the movement of flock of birds, or school of fish.

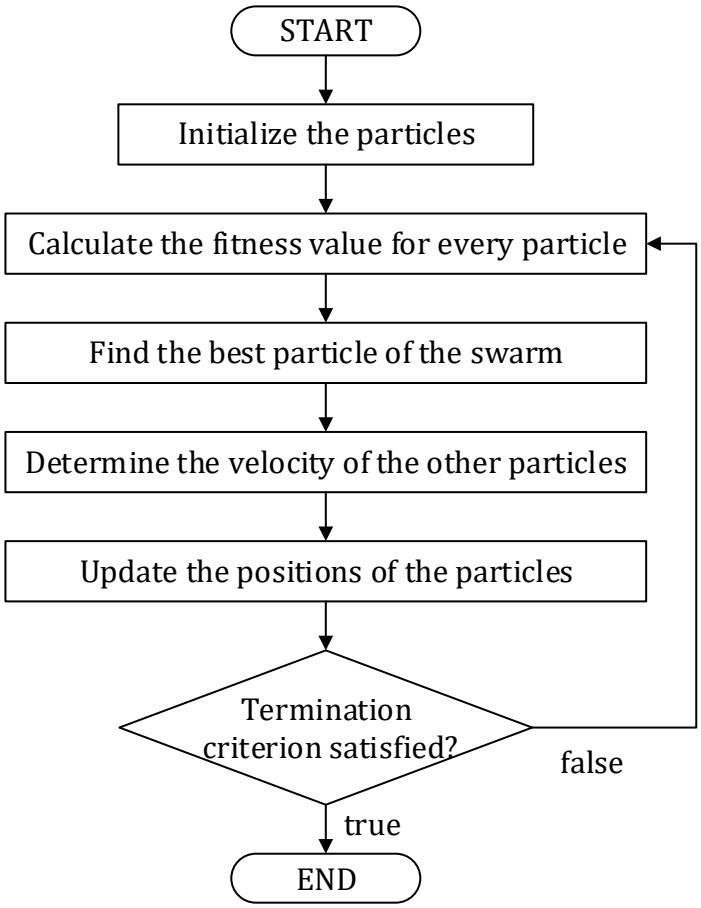

Figure 9 *General flowchart of the particle swarm optimization method*

Figure 9 shows the flowchart of the PSO method used in the determination of the optimum counterbalancing condition. The relatively easy modification of the optimization goal is a great benefit of the presented calculation method. Due to the metaheuristic nature of the method, the global optimum is not guaranteed to be found, but the results are usually better than any other calculation method can provide. Figure 10 shows the determination of the fitness value for each particle, this value determines whether the current configuration is superior to the prior investigated cases.

In the determination of the velocity of each particle both its best position in the calculation and the best position of the swarm in the current iteration step have important role. Using the equation below to find the coordinates of the velocity vector enhances the effectiveness of the PSO calculation method. The constants and the limits of each vector coordinate had been determined based on extensive testing of the procedure on different dynamometer surveys.

$$V_{i+1,j} = W \cdot V_{i,j} + C_1 \cdot Rnd_1 \cdot \left(BP_{i,j} - P_{i,j}\right) + C_2 \cdot Rnd_2 \cdot \left(GBP_i - P_{i,j}\right)$$

where:

$V_{i,j}$	j[th] velocity component of a particle in the i[th] iteration step [-],
W	Damping factor [-],
C_1, C_2	Acceleration coefficients [-],
Rnd_1, Rnd_2	Random numbers from [0,1] [-],

$BP_{i,j}$ j[th] component of the best position of a particle in the i[th] iteration step [-],
$P_{i,j}$ j[th] component of the position of a particle in the i[th] iteration step [-], and
GBP_j j[th] component of the global best position [-].

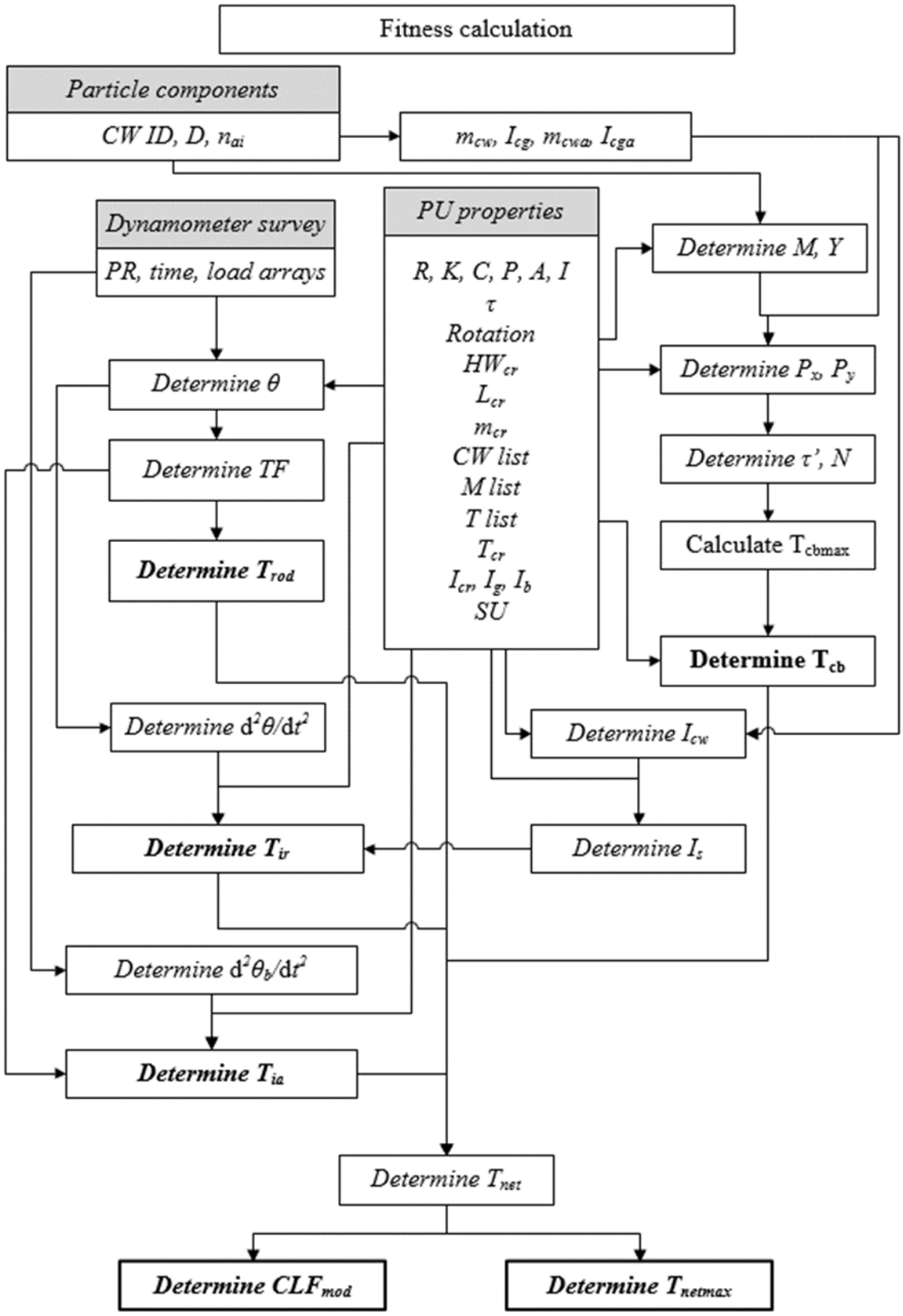

Figure 10 *Flowchart of the fitness calculation*

Figure 11 shows the results of the torque optimization procedure compared to the optimum solution provided by the TAM software; the most relevant properties of the net gearbox torque functions are listed in Table 1.

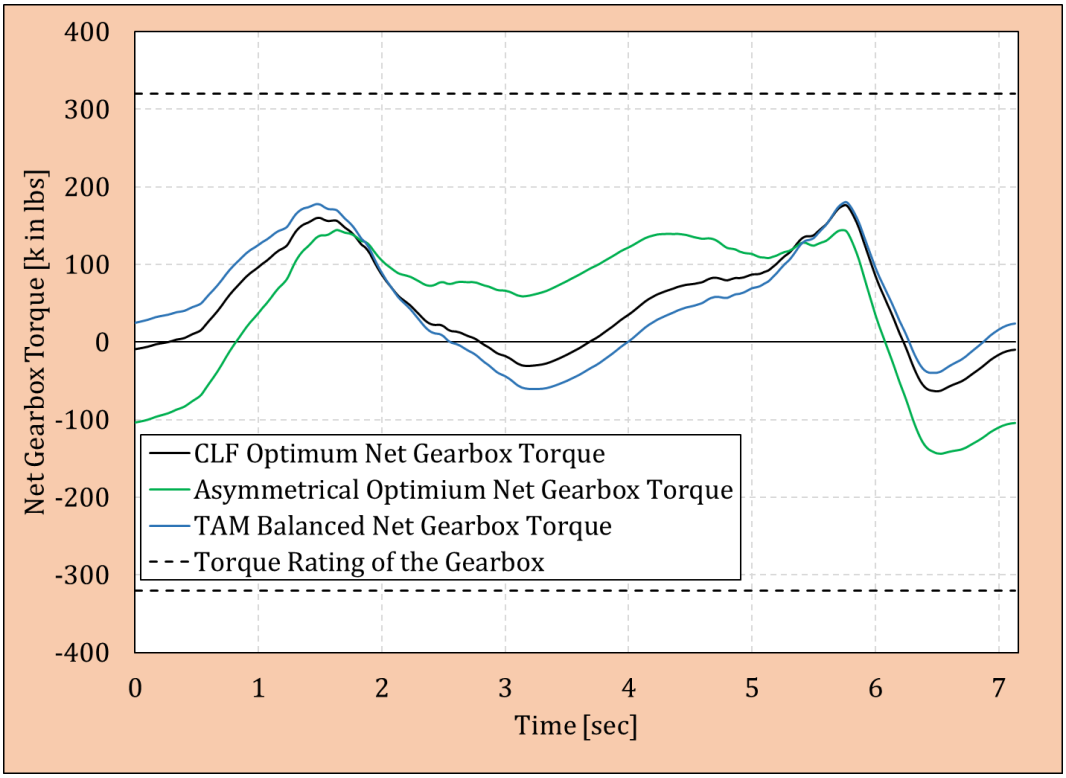

Figure 11 *Comparison of the torque optimization with TAM results*

Table 1 *Summary of the optimization results for the example case*

	Optimization Objective	Peak Net Gearbox Torque [k in lbs]	CLF_{mod} [-]	τ' [deg]
Original Case	-	245.11	1.929	0
TAM Result	Peak Torque	180.10	1.727	0
Results of the Optimization				
Identical Counterweights and Positions	Peak Torque	178.85	1.728	0
No Constraint in the Optimization	Peak Torque	144.33	2.151	-15.22
	CLF_{mod}	176.39	1.625	-4.08
Same Counterweight Configurations on Both Cranks	Peak Torque	178.82	1.728	0

A novel optimization strategy was introduced that considers the gearbox torque rating and the cost of the petroleum production simultaneously. The primary optimization criterion

must be the modified CLF value, since using this scenario the least amount of energy is required to produce the same fluid regime. The peak net gearbox torque must be lower than the rating of the gearbox, or else other optimization goal may be set.

If the overloading of the pumping unit can be prevented by solving the optimization problem using the same main and auxiliary counterweights, the symmetrical optimum counterweight configuration is recommended. However, if the symmetrically placed counterweights cannot reduce the peak net torque below the gearbox torque rating, use of non-identical counterweights can prevent overloading. The proper asymmetrical counterweight configuration will always result in a lower peak net gearbox torque value compared to the symmetrical cases.

THESIS 5

When the sampling rate is low compared to the pumping speed of the unit, the topmost and lowermost polished rod positions may be missing from the dynamometer survey. In such cases, an additional validation step is required to properly calculate crank angles.

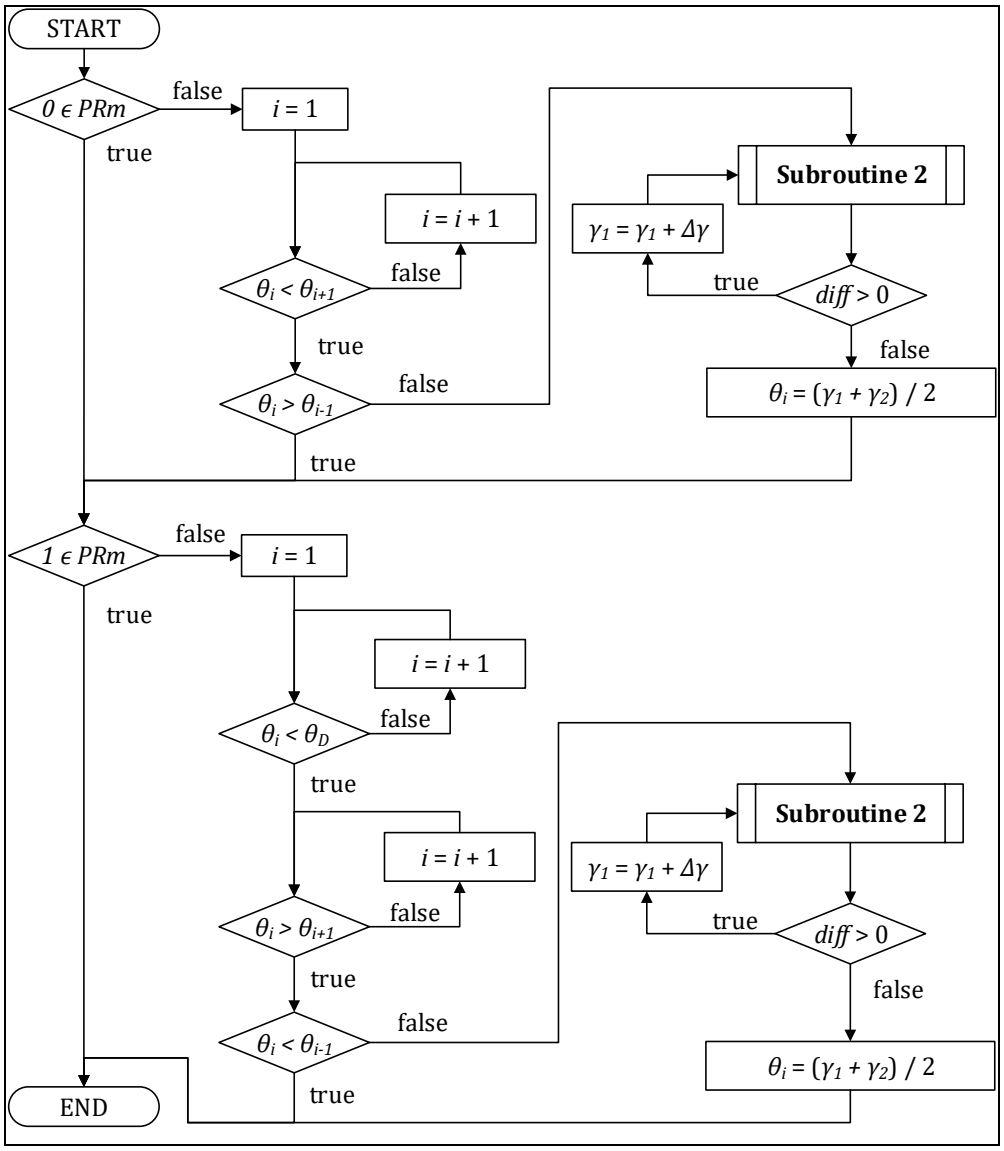

Figure 12 *Flowchart of the improved crank angle calculation procedure*

A new calculation procedure was created to improve the crank angle values in the proximity of the start of the upstroke and downstroke. This validation is required if the dynamometer card does not contain the topmost or lowermost point in the dynamometer survey. By using the proposed method, the incorrect calculation of the crank angle in the wrong pumping phase is prevented, therefore, reducing the error in the determination of the crank angular velocity and crank angular acceleration values. Figure 12 shows the flowchart of the proposed method increasing the accuracy of the crank angle values when interpreting dynamometer surveys with low sampling speeds.

THESIS 6

A modified cyclic load factor – CLF_{mod} – was developed to describe the relative power consumption of the prime mover with a higher accuracy. This new parameter considers the varying crank angular velocity, therefore it gives improved results when a sucker-rod pumping unit is driven by a high slip, or ultra-high slip electric motor.

$$CLF_{mod} = \frac{\sqrt{\frac{\int_{t=0}^{T}\left(T_{net}(t)\right)^2 \mathrm{d}t}{T}}}{\frac{\int_{t=0}^{T} T_{net}(t)\mathrm{d}t}{T}}$$

where:

CLF_{mod}	Modified cyclic load factor [-],
$T_{net}(t)$	Net gearbox torque variation in time [in lb], and
T	Period time of the investigated pumping unit [sec].

The equation used in the past was used mainly because the crank angle was the basis of the torque analysis, every parameter was calculated at equally distributed crank angle values. In these cases, the constant increase of the crank angle function was assumed. The basis of the proposed equation is time; therefore, this new equation is capable to consider the precisely calculated crank angle variation throughout the pumping cycle.

SUMMARY AND POTENTIAL FURTHER RESEARCH DIRECTIONS

The evaluation of the dynamometer survey was improved, compared to the previous publications and software used in the petroleum industry. The first important scientific result is the creation of a high-accuracy calculation method to find the crank angles corresponding to the measured polished rod position values. With these more accurate crank angles, the interpretation of the dynamometer survey and the torque analysis will have smaller errors.

The calculation of the angular acceleration of the crank arm and the walking beam was improved, ensuring the accurate description of the inertial torques during the pumping cycle. Every calculation presented is able to consider the varying crank velocity of pumping units driven by high slip or ultra-high slip prime movers. Several previously published methods, basic numerical methods, and novel calculation procedures were introduced and compared, to provide the variation of the necessary variables in time with the highest accuracy possible. The

application of Fourier series was essential to improve the calculation of the relevant angles and their acceleration pattern during the pumping cycle.

The complete calculation of the actual net gearbox torque variation was detailed while solving an example problem to help the better understanding of the proposed methods. The proper inclusion of the inertial torques can change the net gearbox torque function significantly, as shown in the comparison with the results of the TAM software.

Most importantly, the in-depth investigation of the effect of asymmetrically placed counterweights on the crank arms was carried out. In previous works application of asymmetrically placed counterweights was not advised, because its effect on the net gearbox torque was unknown. The secondary phase angle was defined to describe the lead- or lag of the center of gravity of the system containing the counterweights and the crank from the crank centerline.

Based on the proposed dynamometer survey interpretation, the determination of the optimum net gearbox torque was carried out using two different optimization criteria. A modified cyclic load factor was introduced to improve the efficiency calculation of the sucker-rod pumping units with varying crank angular velocities. In previous works the cases with non-constant crank angular velocities were not taken properly into account. If the pumping unit is overloaded in the best cyclic load factor case, then a different optimization criteria was used to protect the gearbox: the maximum mechanical net gearbox torque.

A particle swarm optimization technique was developed to find the counterweight configuration that produces the optimum torque loading of the gearbox. Using this method, better torque loading was achieved than the results of previously published methods and software used in the industry by considering the asymmetrical counterweight configurations. Using the secondary phase angle as an additional degree of freedom in the optimization procedure, the results were superior compared to the symmetrical counterbalancing cases.

The knowledge of numerous parameters is required by the complete torque analysis, as seen in the proposed thesis. Some of these variables are usually unknown for the production engineers, or would require extensive and expensive measurements to determine their proper values. Several practical equations are introduced to give a reasonable approximation of these parameters enabling the operators of the sucker-rod pumping unit to carry out an in-depth torque analysis and therefore improve the economic value of the installation.

There are possible future research paths based on the introduced calculation procedures. The exact determination of the change in the crank and beam angular acceleration as a function of the net gearbox torque would be a great addition, but it seems unlikely that a general solution exists for this problem.

The incorporation of the proposed asymmetrical counterbalancing calculations in works like (Koncz, 2018) would be beneficial. Using the introduced methods to update the software evaluating the dynamometer surveys could result in more favorable operating conditions for sucker-rod pumping units. The calculation procedure presented can be modified to improve the results of a multi-balance technology introduced in (Feng, et al., 2015).

The method introduced can be modified and applied to sucker-rod pumping units with variable speed drives, further improving their efficiency. For this, however, further study of the complex interactions between the controlled crank angular acceleration pattern by the microcontroller and the resulting net gearbox torque function is needed.

RELEVANT PUBLICATIONS PRESENTED IN THE THESIS' TOPIC

Kis, L. (2013): Calculation of the gearbox torque including inertia effects. Doktoranduszok Fóruma, Conference Proceeding. Miskolc. 46-50

Kis, L. (2014): Comparison of beam acceleration calculation models. XXVIII. MicroCad International Multidisciplinary Scientific Conference, Conference Proceeding. Miskolc

Takács, G., & **Kis, L**. (2014): Finding the best way to calculate articulating torque on sucker-rod pumping gear reducers. *Kőolaj és földgáz*, 2014/3. 17-20.

Kis, L. (2014): A dinamométeres mérések kiértékelésének nehézségei (in Hungarian). Doktoranduszok Fóruma, Conference Proceeding. Miskolc

Takács, G., & **Kis, L.,** & Koncz, Á. (2015): The use of Dynamometer Data for Calculating the Torsional Load on Sucker-Rod Pumping Gearboxes, Southwestern Petroleum Short Course, Texas, 22-23 April, 2015. 176-183.

Kis, L. (2015): Mechanical Net Torque Optimization of Sucker-Rod Pumping Units, XXIX. MicroCad International Multidisciplinary Scientific Conference, Conference Proceeding. Miskolc

Kis, L. (2015): The effect of the articulating inertial torque on the permissible loads of sucker-rod pumping units, *Műszaki Földtudományi Közlemények*, 85(1), 118-122.

Takács, G., & **Kis, L.**, & Koncz, Á. (2016): The calculation of gearbox torque components on sucker-rod pumping units using dynamometer card data. *Journal of Petroleum Exploration and Production Technology*, 101-110. doi: https://doi.org/10.1007/ s13202-015-0172-z

Koncz, Á., & **Kis, L.**, & Szabó, T. (2018): New method for stripper well supervision. 18th International Multidisciplinary Scientific Geoconference SGEM 2018, Conference Proceedings. Sofia, Bulgaria. STEF92 Technology Ltd. 649-656. doi: https://doi.org/ 10.5593/sgem2018/1.4/S06.085

Koncz, Á., & **Kis, L.** (2020). Particle swarm optimization usage in petroleum production, *Műszaki Földtudományi Közlemények*, 89(2), 117-125.

Takács, G., & **Kis, L.** (2021). A New Model to Find Optimum Counterbalancing of Sucker-Rod Pumping Units Including a Rigorous Procedure for Gearbox Torque Calculations, *Journal of Petroleum Science and Engineering*, 205, 108792. https://doi.org/10.1016/ j.petrol.2021.108792

MOST IMPORTANT REFERENCES RELATED TO THE THESIS

API. (2013, November). Specification for Pumping Units. 19th Edition. Washington DC.: American Petroleum Institute.

Clegg, J. (2007). Petroleum Engineering Handbook (Vol. IV). Society of Petroleum Engineers.

Eberhart, R. C., & Kennedy, J. (2001). Swarm Intelligence. Morgan Kaufmann.

Echometer. (2011). Retrieved 04 21, 2020, from http://www.echometer.com/Products/Transducers

Echometer. (2018). Total Asset Monitor Acquisition and Analysis Operating Manual. Wichita Falls, Texas: Echometer Company.

Engelbrecht, A. (2007). Computational Intelligence. John Wiley & Sons, Ltd.

Gibbs, S. G. (1975, September). Computing Gearbox Torque and Motor Loading for Beam Pumping Units with Consideration of Inertia Effects. Journal of Petroleum Technology, 1153-1159.

Koncz, Á. (2018). Sucker Rod Pumping Analysis Based on Measured Electrical Parameters, PhD Thesis.

Lea, F. (2007). Artificial Lift Selection, Chapter 10. In Petroleum Engineering Handbook (Vol. IV.). Dallas, Texas: Society of Petroleum Engineers.

Lufkin. (1997). Conventional Counterbalance Torque (CBT) Data.

Rowlan, O., McCoy, J., & Podio, A. (2005, July). Best Method to Balance Torque Loadings on a Pumping Unit Gearbox. Journal of Canadian Petroleum Technology, 44(07), 27-33. doi:https://doi.org/10.2118/05-07-TN3

Schlumberger. (2019). Sucker Rod Pump Surface Units Catalog. Schlumberger.

Svinos, J. G. (1983). Exact kinematic analysis of pumping units. 58th Annual Technical Conference and Exhibition of the SPE. SPE 012201-MS. San Francisco, California: Society of Petroleum Engineers.

Takács, G. (1989). Torque analysis of pumping units using dynamometer cards. Proc. 36th Annual Southwestern Petroleum Short Course, (pp. 366-376). Lubbock, Texas.

Takács, G. (2015). Sucker-Rod Pumping Handbook. Elsevier.

Takács, G., Kis, L., & Koncz, Á. (2016). The calculation of gearbox torque components on sucker-rod pumping units using dynamometer card data. Journal of Petroleum Exploration and Production Technology, 101-110. doi:https://doi.org/10.1007/s13202-015-0172-z